Finite element approximation of 3D non-hydrostatic turbulent coastal ocean flows using a LES model

Jordi Blasco[⋆,(1)], M. Augusto Maidana[(2)], Arnel German[(2)], Manuel Espino[(2)]

(1) Departament de Matemàtica Aplicada I, Univ. Politècnica de Catalunya, Campus Sud, Edifici H, Avgda. Diagonal 647, 08028, Barcelona, Spain.

(2) Laboratorio de Ingeniería Marítima, Univ. Politècnica de Catalunya Campus Nord, Edfici D1, c/Gran Capità s/n, 08034 Barcelona (Spain)

Abstract

In this paper we present a stabilized finite element method for three-dimensional, non-hydrostatic, turbulent coastal ocean flows. The model we have developed, named HELIKE, incorporates also surface wind stress, bottom friction, Coriolis forces and several closure models for both the horizontal and the vertical turbulent eddy viscosity coefficients. Unstructured meshes are employed so that complex geometries can be accurately approximated, and implicit time stepping allows to use large time steps. Numerical results are presented in various test cases, in which comparisons between different turbulence models are provided.

Key words: Ocean modelling, Non-hydrostatic flows, Navier-Stokes equations, Finite elements, Turbulence modelling

⋆ This author's work was partially supported by the Spanish MEC under Projects MTM2005-07660-C02-01 and BFM2003-06446-C02-02.

Email addresses: jorge.blasco@upc.edu (Jordi Blasco), augusto.maidana@upc.edu (M. Augusto Maidana), arnel.german@upc.edu (Arnel German), manuel.espino@upc.edu (Manuel Espino).

URL: http://www.ma1.upc.edu/~blasco (Jordi Blasco).

1 Introduction

A large number of numerical models for the simulation of coastal and shelf sea flows are available nowadays. Old versions were based on simplified equations derived under the hydrostatic pressure approximation, like shallow water models (see [17], [20], [36], [39] and [48], for instance) or primitive equation models (see [11], [16] and [25], among several others). However, non-hydrostatic models are able to reproduce effects which can be important is some situations, such as flows over rapidly varing slopes.

The finite difference method has been classically used in most coastal ocean models. But the finite element method (FEM) provides more flexibility to approximate the complex geometry of coastlines and bathimetries, especially when combined with unstructured meshes. Also, three-dimensional models are affordable nowadays due to the availability of computer power resources. Non-hydrostatic, three-dimensional, finite element coastal models have been presented in [10], [31] and [45]. In [7] the model named HELIKE was introduced, which is also a 3D, non-hydrostatic, finite element model that employs a pressure stabilized formulation and an implicit time-stepping scheme.

One of the main difficulties of simulating coastal and shelf sea flows is the modelling of turbulence and the effects of subgrid scales of motion. The prohibitive cost of direct numerical simulations (DNS) of turbulent transient coastal ocean flows drives the strong interest for simplified models, which are less expensive from a computational point of view but still relevant in properly describing the largest scales of the ocean flow (long and mesoscale currents). In the past (and still nowadays), much of the mathematical modelling of ocean flows on various scales was based on simple assumptions about the turbulent eddy viscosity coefficients, which were often taken to have constant values, chosen to give the best agreement with observations. Though the preoccupation with finding numerical values of these parameters was not in retrospect always helpful, certain features of those results contained the seeds of many real developments in this subject. The horizontal and vertical mixing coefficients evaluated this way differ by many orders of magnitude, and it was soon recognized that the much smaller rates of vertical mixing must in same way be due to the smaller scale of the vertical ocean motions. Qualitatively, it was also known that the vertical eddy coefficients tended to be smaller when the density vertical gradients were larger.

Furthermore, realistic horizontal ocean flow fields are almost always characterized by the presence of coastlines of quite complex geometry. The presence of these boundaries affects the kinetics of the flow through several mechanisms, one of them being the presence of a strong shear that usually peaks at the boundary and is responsible for the production of streamwise vortices and

streaky structures that eventually detach and sustain the turbulent fluctuations in the bulk. Among the simplified models which have been developed to account for these turbulent fluctuations is the Large-Eddy Simulation or LES, in which the largest scales of motion, responsible for the momentum, matter and energy ocean transport, are computed and only the small scales, which are generally more homogeneous and isotropic (and, therefore, easier to model) are parametrized. The effect of the small subgrid scales appears in the governing equations for LES through an additional stress term, which must be modelled. Moreover, the Smagorinsky parametrization (see [43]) is the most extensively used LES formulation. The variational multiscale method initially designed for the development of stabilized numerical schemes (see [27], [28]) has been shown to be closely related to the Smagorinsky LES turbulence model (see [2], [29] and the references therein). In the present work we consider the Smagorinsky model for the calculation of the horizontal eddy viscosity coefficient.

On the other hand, the presence of a homogeneous vertical layer near the surface of the ocean, named mixed layer, which presents almost constant density profiles is also well known. The bottom of this mixed layer corresponds to the top of the pycnocline, a zone of large gradients of density. Most vertical ocean subgrid-scale models have been derived to describe the vertical turbulent distribution of this ocean mixing boundary layer. These models span the range from simple prescribed values for the vertical turbulent diffusivities up to complex Reynolds-stress models with several differential transport equations to solve. In this paper, we consider three different versions of the family of algebraic vertical turbulent models, defined in terms of the Richardson number which determines the stability of vertical ocean layers through the ratio between buoyancy and inertia forces in these layers.

The paper is organized as follows: in Section 2 the mathematical problem considered is described, while in Section 3 the different turbulence closure models that we use are presented. Section 4 is dedicated to the numerical method employed to solve the problem, and numerical results are presented in Section 5 where comparisons between the performance of the different turbulence formulations on test problems are given. Finally, some conclusions are drawn.

2 Problem statement and notation

Our objective is the study of the dynamics of water in coastal regions such as bays, river mouths, beaches or harbors. The domain of interest, which is assumed to be occupied by an incompressible fluid, can be represented as:

$$\Omega = \{(x, y, z) \in \mathbb{R}^3 \ / \ (x, y) \in S, \ -H(x, y) < z < 0\}$$

referred to Cartesian coordinates x, y (horizontal, with positive x eastbound and positive y northbound) and z (vertical), where $S \subset \mathbb{R}^2$ is the reference fluid surface (lying in the plane $z = 0$) and $H\colon \bar{S} \to \mathbb{R}$ is a positive function representing the bathymetry. We express the boundary of Ω as $\partial\Omega = \Gamma_s \cup \Gamma_b \cup \Gamma_l$, where:

$$\begin{aligned}
\Gamma_s &= S \times 0 && : \text{the surface,}\\
\Gamma_b &= \{(x,y,z) \in \mathbb{R}^3 \,/\, (x,y) \in S,\, -H(x,y) = z\} && : \text{the bottom,}\\
\Gamma_l &= \{(x,y,z) \in \mathbb{R}^3 \,/\, (x,y) \in \partial S,\, -H(x,y) \le z \le 0\} && : \text{the lateral boundary.}
\end{aligned}$$

The governing equations considered are the three-dimensional, incompressible Navier-Stokes equations, expressed in a rotating coordinate system and under the Boussinesq assumption. These equations accomodate a wide range of temporal and spatial scales, from mean currents down to dissipation scales for turbulence. Since it is not feasible to solve them over all scales, ocean models are usually based on some form of averaging (filtering) of the original equations, which can be temporal (as in the Reynolds averaged Navier-Stokes equations or RANS), spatial (as in Large Eddy Simulation or LES models) or statistical averaging. The Reynolds stress tensor is subsequently modelled in terms of eddy viscosities; due to the spatial anisotropy of the ocean, the mixing of motion need not be the same in the horizontal than in the vertical directions, so that different viscosity coefficients are considered for horizontal and vertical turbulence. The mathematical problem considered here is, thus, the following (see [42]):

$$\begin{aligned}
\frac{\partial \boldsymbol{u}}{\partial t} + (\boldsymbol{u}\cdot\nabla)\boldsymbol{u} + \boldsymbol{k}\times\boldsymbol{u} + \nabla P - \frac{\partial}{\partial x}(\nu_H \frac{\partial \boldsymbol{u}}{\partial x}) - \frac{\partial}{\partial y}(\nu_H \frac{\partial \boldsymbol{u}}{\partial y}) - \frac{\partial}{\partial z}(\nu_V \frac{\partial \boldsymbol{u}}{\partial z})\\
= -\frac{\rho}{\rho_0}\boldsymbol{g} \qquad \text{in } \Omega \times (0,T), \qquad (1)\\
\nabla \cdot \boldsymbol{u} = 0 \qquad \text{in } \Omega \times (0,T). \qquad (2)
\end{aligned}$$

In (1)-(2), $\boldsymbol{u} = (u, v, w)$ is the three-dimensional velocity of the fluid (as usual, boldface characters denote vector fields) and $P(x, y, z, t)$ is the fluid kinematic pressure, that is, the pressure divided by a reference fluid density ρ_0; the unknowns $\boldsymbol{u}$ and P are functions of the spatial coordinates $(x, y, z) \in \Omega$ and time $t \in (0, T)$, with $T > 0$ a given final time. Moreover, $\nabla = (\frac{\partial}{\partial x}, \frac{\partial}{\partial y}, \frac{\partial}{\partial z})$ is the three-dimensional gradient operator and $\boldsymbol{k} = (0, b, f)$, where $f = 2\boldsymbol{\omega}\sin(\phi)$ and $b = 2\boldsymbol{\omega}\cos(\phi)$ are the normal and tangential Coriolis parameters, respectively, ω is the Earth's angular velocity and ϕ the latitude of the region of interest (the tangential component of the Coriolis acceleration should be retained in non-hydrostatic models, see [35]). Furthermore, ν_H and ν_V are the horizontal and vertical turbulent eddy viscosities, respectively. We are using

a prognostic model in which the fluid density ρ is assumed to be known. Finally, $\boldsymbol{g} = (0, 0, g)$, where g is the gravitational acceleration; centrifugal accelerations have been incorporated into the gravity term, yielding an effective gravity acceleration which is aligned with the vertical axis.

In order to account for variations of the fluid surface position, it is usual in ocean models to consider a function $\eta(x, y, t)$, with $(x, y) \in S$ and $t \in (0, T)$, which represents the free-surface elevation with respect to the reference level $z = 0$. Since the magnitude of η is small compared to the ocean's depth, the hydrodynamical problem is solved in the fix domain Ω. The free-surface elevation η satisfies the kinematic equation:

$$\frac{\partial \eta}{\partial t} + u \frac{\partial \eta}{\partial x} + v \frac{\partial \eta}{\partial y} = w \quad \text{in } S \times (0, T). \tag{3}$$

Furthermore, the total pressure P in equation (1) can be decomposed into its atmospheric, barotropic, baroclinic and non-hydrostatic components, as:

$$P(x, y, z, t) = p_a(x, y, t) + g(\eta - z) + g \int_z^\eta \frac{\rho - \rho_0}{\rho_0} ds + p(x, y, z, t), \tag{4}$$

where p_a is the atmospheric pressure (which from now on we assume to be zero) and p is the non-hydrostatic part of the pressure. Using (4) in (1) results in:

$$\frac{\partial \boldsymbol{u}}{\partial t} + (\boldsymbol{u} \cdot \nabla)\boldsymbol{u} + \boldsymbol{k} \times \boldsymbol{u} + \nabla p - \frac{\partial}{\partial x}(\nu_H \frac{\partial \boldsymbol{u}}{\partial x}) - \frac{\partial}{\partial y}(\nu_H \frac{\partial \boldsymbol{u}}{\partial y}) - \frac{\partial}{\partial z}(\nu_V \frac{\partial \boldsymbol{u}}{\partial z})$$
$$= -g \nabla_2 \eta - \frac{g}{\rho_0} \nabla_2 (\int_z^\eta \rho \, ds) \qquad \text{in } \Omega \times (0, T), \tag{5}$$
$$\nabla \cdot \boldsymbol{u} = 0 \qquad \text{in } \Omega \times (0, T), \tag{6}$$

where $\nabla_2 = (\frac{\partial}{\partial x}, \frac{\partial}{\partial y}, 0)$ is the two-dimensional gradient operator extended to 3D. The model that we propose is based on the momentum equation (5), the continuity equation (6) and the kinematic free-surface equation (3). It remains to specify a turbulence closure model for the computation of the eddy viscosity coefficients ν_H and ν_V, which will be considered in the next Section.

Boundary conditions have to be supplied to the equation system (5)-(6)-(3) which should reflect different physical boundary phenomena acting on the fluid. We consider an impermeable bottom Γ_b through which no mass flux occurs; also, a linear model for bottom friction due to rugosity is considered on Γ_b. At the fluid surface Γ_s, wind stress is modelled by the usual quadratic dependence law on the wind velocity and zero normal stress is also imposed. Finally, in the lateral boundary Γ_l different situations are considered, such as solid walls (Γ_w), inflow (Γ_i) and outflow regions (Γ_o). The boundary conditions for (5)-(6)-(3) are, thus, the following:

$$w \;+\; u\frac{\partial H}{\partial x} \;+\; v\frac{\partial H}{\partial y} = 0 \quad \text{on } \Gamma_b, \tag{7}$$

$$\nu_H\, n_x(\frac{\partial u}{\partial x}, \frac{\partial v}{\partial x}) + \nu_H\, n_y(\frac{\partial u}{\partial y}, \frac{\partial v}{\partial y}) + \nu_V\, n_z(\frac{\partial u}{\partial z}, \frac{\partial v}{\partial z}) = \tag{8}$$

$$(\tau_b^x, \tau_b^y) \;:=\; C_b(u, v) \qquad \text{on } \Gamma_b,$$

$$\nu_V(\frac{\partial u}{\partial z}, \frac{\partial v}{\partial z}) = \tag{9}$$

$$(\tau_s^x, \tau_s^y) \;:=\; \frac{\rho_a}{\rho_0} C_s (U_{10}^2 + V_{10}^2)^{1/2}(U_{10}, V_{10}) \qquad \text{on } \Gamma_s,$$

$$\nu_V \frac{\partial w}{\partial z} = 0 \quad \text{on } \Gamma_s, \tag{10}$$

$$n_x\, u \;+\; n_y\, v = 0 \quad \text{on } \Gamma_{\mathrm{w}}, \tag{11}$$

$$\boldsymbol{u} = \boldsymbol{u}_i \;\; \text{on } \Gamma_{\mathrm{i}}, \tag{12}$$

$$\nu_H\, n_x\, \frac{\partial \boldsymbol{u}}{\partial x} \;+\; \nu_H\, n_y\, \frac{\partial \boldsymbol{u}}{\partial y} = \boldsymbol{0} \quad \text{on } \Gamma_{\mathrm{o}}. \tag{13}$$

Here, $\boldsymbol{n} = (n_x, n_y, n_z)$ is the unit outward normal vector to Γ, C_b is the linear bottom friction coefficient, ρ_a is the air's density, C_s the dimensionless wind drag coefficient, (U_{10}, V_{10}) is the horizontal wind velocity vector at a reference height of 10 m above the surface and $\boldsymbol{u}_i$ is a given inflow velocity.

An initial condition must also be specified for the velocity field:

$$\boldsymbol{u}(x, y, z, 0) \;=\; \boldsymbol{u}^0(x, y, z), \quad \forall (x, y, z) \in \Omega, \tag{14}$$

where $\boldsymbol{u}^0$ is a given three-dimensional, divergence-free initial velocity.

The hydrodynamical model that we consider consists of equations (3), (5) and (6), boundary conditions (7)–(13) and the initial condition (14). In order to write down the weak form of this problem, which will be needed when we introduce its finite element approximation, and just for simplicity of exposition, we will assume in what follows that $\Gamma_l = \Gamma_{\mathrm{i}}$ and $\boldsymbol{u}_i = \boldsymbol{0}$, that is to say, that in the lateral boundary only homogeneous Dirichlet boundary conditions are specified. Then, the velocity $\boldsymbol{u}$, the non-hydrostatic pressure p and the free-surface elevation η belong, respectively, to the following spaces:

$$V := \Big\{ \tilde{\boldsymbol{u}} = (\tilde{u}, \tilde{v}, \tilde{w}) \in \boldsymbol{H}^1(\Omega) : \tilde{\boldsymbol{u}} = \boldsymbol{0} \,\text{on}\, \Gamma_{\mathrm{i}},\; \tilde{w} + \tilde{u}\frac{\partial H}{\partial x} + \tilde{v}\frac{\partial H}{\partial y} = 0 \,\text{on}\, \Gamma_b \Big\}$$

$$Q := L^2(\Omega)$$

$$M := H^1(S)$$

The weak form of the momentum equation (5), the continuity equation (6) and the free-surface equation (3) can be written, for adequate test functions $\tilde{\boldsymbol{u}} = (\tilde{u}, \tilde{v}, \tilde{w}) \in V$, $q \in Q$ and $\mu \in M$, as:

$$
\begin{aligned}
\int_\Omega \frac{\partial \boldsymbol{u}}{\partial t}\,\tilde{\boldsymbol{u}}\,d\Omega + \int_\Omega (\boldsymbol{u}\cdot\nabla)\boldsymbol{u}\,\tilde{\boldsymbol{u}}\,d\Omega \;+\; \int_\Omega (\boldsymbol{k}\times\boldsymbol{u})\,\tilde{\boldsymbol{u}}\,d\Omega \;+\; \int_\Omega \nabla p\,\tilde{\boldsymbol{u}}\,d\Omega \\
+ \int_\Omega \Big(\nu_H \frac{\partial \boldsymbol{u}}{\partial x}\frac{\partial \tilde{\boldsymbol{u}}}{\partial x} + \nu_H \frac{\partial \boldsymbol{u}}{\partial y}\frac{\partial \tilde{\boldsymbol{u}}}{\partial y} + \nu_V \frac{\partial \boldsymbol{u}}{\partial z}\frac{\partial \tilde{\boldsymbol{u}}}{\partial z}\Big)\,d\Omega \\
= -g\int_\Omega \nabla_2\eta\,\tilde{\boldsymbol{u}}\,d\Omega \;-\; \frac{g}{\rho_0}\int_\Omega \nabla_2\Big(\int_z^\eta \rho\,ds\Big)\,\tilde{\boldsymbol{u}}\,d\Omega \\
+ \int_{\Gamma_s} (\tau_s^x\tilde{u} + \tau_s^y\tilde{v})\,d\Gamma \;+\; \int_{\Gamma_b} (\tau_b^x\tilde{u} + \tau_b^y\tilde{v})\,d\Gamma \\
+ \int_{\Gamma_b} \boldsymbol{n}_\nu\cdot\nabla w\,\tilde{w}\,d\Gamma,
\end{aligned}
$$

$$
\int_\Omega (\nabla\cdot\boldsymbol{u})\,q\;d\Omega \;=\; 0,
$$

$$
\int_S \frac{\partial \eta}{\partial t}\,\mu\,d\Gamma \;+\; \int_S u\,\frac{\partial \eta}{\partial x}\,\mu\,d\Gamma \;+\; \int_S v\,\frac{\partial \eta}{\partial y}\,\mu\,d\Gamma \;=\; \int_S w\,\mu\,d\Gamma,
$$

where (τ_b^x, τ_b^y) are given by (8) and (τ_s^x, τ_s^y) by (9) and we have used the notation $\boldsymbol{n}_\nu = (\nu_H n_x, \nu_H n_y, \nu_V n_z)$.

3 Turbulence closure models

The parametrization of the physical processes of horizontal and vertical diffusion of momentum is one of the most complex problems in ocean modelling. These processes are characterized by the horizontal (ν_H) and the vertical (ν_V) eddy viscosity coefficients, the value of which has to be determined by an adequate turbulence model. A large number of such techniques have been developed so far, ranging from simple algebraic models to (one and two) differential equation models. We will focus our attention here only on algebraic models for their simplicity and efficiency and because their use is well established in ocean modelling; other areas of Physics such as channel flows may need more elaborate turbulence models, but algebraic models are sufficient for ocean flow simulations. Comparisons between different turbulence closure models in ocean flows were given in [4], [15] and [46], the conclusion being that simple flow dependent eddy viscosity models perform as well as more complex schemes.

3.1 Horizontal turbulent viscosity

The simplest possibility for the determination of the horizontal turbulent viscosity coefficient ν_H is to use a constant value, a choice which is present in many ocean models (see [9], [10], [16], [31] and [47], for instance). Estimates

indicate that this value should be in the range 10^1-10^4 m^2/s for the ocean (see [42]).

However, the most extensively used formulation for ν_H in ocean models is the Smagorinsky parametrization (see [43]). This is an LES formulation which is employed, among others, in well known coastal models such as POM ([8]) and ROMS ([26]) and also in [24], for instance. In this formulation, the coefficient ν_H is determined as:

$$\nu_H \;=\; C_{m_0}\, h_x\, h_y\, D_T,$$

where C_{m_0} is an adimensional Smagorinsky viscosity coefficient, h_x and h_y are the sizes of the horizontal discretization employed in the x and y directions, respectively, and:

$$D_T \;=\; (\,(\partial_x u)^2 \;+\; (\partial_y v)^2 \;+\; \frac{1}{2}(\partial_y u + \partial_x v)^2\,)^{1/2},$$

is the magnitude of the velocity of strain tensor. The adimensional parameter C_{m_0} can be determined empirically; Smagorinsky ([44]) provides several theories for the selection of C_{m_0} for isotropic, homogeneous three-dimensional turbulence. The suggested range for this coefficient is $0.1 \leq C_{m_0} \leq 0.2$; we take $C_{m_0} = 0.1$ in our model.

The turbulent viscosity introduced by the Smagorinsky model increases in regions where the horizontal shear stress is important, for instance near the boundary. On the contrary, it decreases in regions of small velocity variations, like in the interior of the ocean. In general, this approximation produces sufficient viscosity in areas with large velocity of the current, but it may underdissipate in areas with smaller velocities (see [24]).

3.2 Vertical turbulent viscosity

There is not such agreement on a single model for the vertical turbulent viscosity coefficient ν_V as there is for the Smagorinsky model in the horizontal. Once again, a constant value is the simplest choice for vertical turbulence, a possibility which is considered, for instance, in [9], [10], [16], [31] and [47]. Adequate values for which have been estimated to be in the range 10^{-4}-10^{-1} m^2/s (see [42]). A two-layer mixing length model for the vertical eddy viscosity ν_V was considered in [30]. More complex, and therefore computationally more expensive, schemes like the $k-\epsilon$ and the $k-l$ models have also been employed (see [34]).

However, the main factors which induce the development of turbulence in the vertical direction of the ocean are buoyancy forces and shear stresses. The models proposed for ν_V should reflect these physical effects. This is the

reason why most of the existing algebraic models are defined in terms of the Richardson number:

$$R_i \;:=\; N^2 \,/\, M^2,$$

which determines the stability of fluid layers by expressing the ratio between buoyancy and inertia forces. Here, N^2 is the frequency of the vertical oscillations (also called stratification frequency or Brunt-Väisälä frequency, see [41]) given by:

$$N^2 \;=\; -\frac{g}{\rho_0}\,\frac{\partial \rho}{\partial z},$$

which is related to buoyancy, and M^2 is given in terms of the vertical gradient of the horizontal velocities as:

$$M^2 \;=\; (\frac{\partial u}{\partial z})^2 \;+\; (\frac{\partial v}{\partial z})^2.$$

The different flow dependent models for the vertical turbulent viscosity can all be written as:

$$\nu_V \;=\; \nu_0 \;+\; \frac{\nu_1}{(1 \;+\; \beta R_i)^n}$$

for different values of the parameters ν_0, ν_1 (both of which have the same units as ν_V, for instance, m^2/s), β and n.

One of the most extensively used expressions for ν_V in ocean flows is the Pacanowski-Philander model (see [40]), which corresponds to the values $n = 2$, $\beta = 5$, $\nu_0 = 10^{-4}$ and $\nu_1 = 10^{-2}$, yielding:

$$\nu_{V,P} \;=\; 10^{-4} \;+\; \frac{10^{-2}}{(1 \;+\; 5R_i)^2}.$$

This formulation was originally developed to be used in oceanographic applications at global scale and has the advantage of being less sensitive to the vertical grid resolution than more advanced turbulence closure models. In the absence of estratification, the coefficient ν_V takes uniform values.

Another model which is frequently used is that of Munk and Anderson (see [37]), which is a classical empirical formulation. It corresponds to the values $n = 0.5$, $\beta = 10$, $\nu_0 = 10^{-4}$ and $\nu_1 = 6 \cdot 10^{-2}$, yielding:

$$\nu_{V,M} \;=\; 10^{-4} \;+\; \frac{6 \cdot 10^{-2}}{\sqrt{1 \;+\; 10R_i}}.$$

Another formulation has recently been proposed by Gent (see [22]) which has also been considered in [32]. This time, the parameters for the vertical turbulent viscosity are the same as in the Pacanowski-Philander model, except for β which is taken as 10 (other differences in the two models are encountered

in the parametrization of the vertical turbulent coefficient for the diffusion of tracers); this results in:

$$\nu_{V,G} \;=\; 10^{-4} \;+\; \frac{10^{-2}}{(1 \,+\, 10 R_i)^2}.$$

In all cases, and in order to avoid an excessive grow of turbulence in the case of unstable estratification ($R_i < 0$), an upper limit for ν_V is imposed. A comparison of the numerical performance of some of these turbulence models and an analytical study of them has been recently given in [3]. In our model we have incorporated the Pacanowski-Philander's, Munk-Anderson's and Gent's models as well as a constant value for ν_V.

4 Numerical approximation

We describe in this Section the numerical scheme that we employ for the approximation of the hydrodynamical problem (3)-(5)-(6). We first introduce the time stepping scheme in a semidiscrete (continuous in space) context and then we consider a spatial discretization by the finite element method.

4.1 Time stepping

We employ here an implicit backward Euler monolithic method for the time integration of (5)-(6) in which the velocity and the pressure are computed simultaneously (a monolithic time stepping method was also employed in [31]). The free-surface elevation, however, is treated explicitly in the momentum equation (5) so as not to increase the dimension of the discrete equation system, and it is updated at the end of the step using the new velocity field just calculated, integrating (3) implicitly once again by the backward Euler method (a similar approach was used in [18] for the treatment of the free-surface elevation).

Thus, given a time step size $\Delta t > 0$ and assuming known an approximation $\boldsymbol{u}^n$ of the velocity and an approximation η^n of the free-surface elevation at time $t_n \,=\, n\,\Delta t$, a new velocity $\boldsymbol{u}^{n+1}$ and pressure p^{n+1} at t_{n+1} are computed

as:

$$\frac{1}{\Delta t}(\boldsymbol{u}^{n+1}-\boldsymbol{u}^{n})\;+\;(\boldsymbol{u}^{n}\cdot\nabla)\boldsymbol{u}^{n+1}\;+\;\boldsymbol{k}\times\boldsymbol{u}^{n+1}+\;\nabla p^{n+1}$$

$$-\frac{\partial}{\partial x}(\nu_H\frac{\partial \boldsymbol{u}^{n+1}}{\partial x})\;-\;\frac{\partial}{\partial y}(\nu_H\frac{\partial \boldsymbol{u}^{n+1}}{\partial y})-\frac{\partial}{\partial z}(\nu_V\frac{\partial \boldsymbol{u}^{n+1}}{\partial z})=-g\,\nabla_2\eta^{n}\text{in }\Omega, \quad (15)$$

$$\nabla\cdot\boldsymbol{u}^{n+1}\;=\;0 \qquad \text{in }\Omega. \quad (16)$$

Once $\boldsymbol{u}^{n+1}$ is known, a new approximation η^{n+1} of the free-surface elevation at time t_{n+1} is obtained implicitly from:

$$\frac{1}{\Delta t}\,(\eta^{n+1}\;-\;\eta^{n}\,)\;+\;u^{n+1}\,(\frac{\partial\eta}{\partial x})^{n+1}\;+\;v^{n+1}\,(\frac{\partial\eta}{\partial y})^{n+1}\;\;=\;\;w^{n+1}\quad\text{in }S. \quad (17)$$

4.2 Finite element spatial approximation

The semidiscrete problem (15)-(16)-(17) is further discretized in space by the finite element method. It is generally agreed that this discretization method presents several advantages over the classical finite difference method still commonly used in ocean modelling (see [9], [30], [33] and [47], for instance), such as flexibility to approximate the domain, mass conservation and natural imposition of boundary conditions. The use of unstructured meshes is highly advisable when solving ocean flows. In our model, whenever barotropic or baroclinic terms are active, we use prismatic finite elements with the nodes arranged in vertical columns; the three-dimensional mesh Ω_h is constructed starting from a two-dimensional, unstructured triangular mesh Σ_h of the surface S, and beneath each triangle an arbitrary number of prismatic elements is allowed. In situations where both barotropic and baroclinic effects can be neglected, we may use fully unstructured three-dimensional meshes Ω_h of tetrahedral or hexahedral finite elements. In all cases, this meshing strategies provide full flexibility to approximate both the coastline and the bottom topography. We assume, moreover, that each element $K\in\Omega_h$ is the image of a reference element $\hat{K}$ by a mapping:

$$F_K\colon \hat{K}\to K \;\text{ with }\; F_K\in(R_1)^3.$$

Here, R_1 is the space of lineal polynomials in the reference variables $(\hat{x},\hat{y},\hat{z})\in\hat{K}$, if $\hat{K}$ is the simplex in $\mathbb{R}^3$ and the elements are tetrahedral; R_1 is the space of lineal polynomials in each reference variable, if $\hat{K}$ is the cube $[-1,1]^3$ and the elements are hexahedral; and R_1 is the tensor product space of linear polynomials in $(\hat{x},\hat{y})$ and $\hat{z}$, when $\hat{K}=\hat{T}\times[-1,1]$ is the reference prism, $\hat{T}$ being the simplex in $\mathbb{R}^2$, and the elements are prismatic.

The unknowns of the problem are approximated by finite element functions,

which are continuous across interelement boundaries. We will focus our attention on the case of equal interpolation for the velocity and the pressure, in which both variables are approximated on the same three-dimensional mesh by polynomials of the same degree. Whenever barotropic effects are considered, the free-surface elevation is approximated by piecewise linear polynomials on the two-dimensional mesh Σ_h. Thus, the finite element spaces for the approximation of the velocity, the pressure and the free-surface elevation are, respectively:

$$
\begin{aligned}
V_h &:= \{\tilde{\boldsymbol{u}}_h \in V \quad / \ \forall K \in \Omega_h,\ \tilde{\boldsymbol{u}}_{h|K} = \hat{\boldsymbol{u}}_K \circ F_K^{-1},\ \hat{\boldsymbol{u}}_K \in (R_1)^3\} \\
Q_h &:= \{q_h \in \mathcal{C}^0(\Omega) \ / \ \forall K \in \Omega_h,\ q_{h|K} = \hat{q}_K \circ F_K^{-1},\ \hat{q}_K \in R_1\} \\
M_h &:= \{\mu_h \in \mathcal{C}^0(S) \ / \ \forall T \in \Sigma_h,\ \mu_{h|T} = \hat{\mu}_T \circ F_T^{-1},\ \hat{\mu}_T \in S_1\}
\end{aligned}
$$

where $F_T \colon \hat{T} \to T$ denotes the linear transformation from $\hat{T}$ onto triangle T and S_1 is the space of linear polynomials in $(\hat{x}, \hat{y})$.

The incompressibility constraint (6) on the velocity field poses a severe problem on the treatment of the pressure. It is well known that if standard approximations are employed in incompressible flow problems, the approximating spaces for the velocity and the pressure have to satisfy a compatibility condition, known as LBB or inf-sup condition, in order to yield a stable and convergent method. It has to be said that equal order interpolations do not satisfy this compatibility condition. Several combinations of finite element spaces for the velocity and the pressure have been developed which do satisfy it, but stabilized formulations which do not require a compatibility condition have proved to be more efficient than stable mixed pairs. In this alternative approach, some terms are added to the discrete problem which enhance its stability.

A stabilized, finite element formulation for steady incompressible flow problems was developed and analyzed in [12] and [13] and extended to the transient case in [6] and [14] (see also [5] for an extension of this technique to anisotropic finite element meshes). The main idea of this method consists in introducing a new unknown of the problem which is the orthogonal projection of the gradient of the discrete pressure onto the space of finite element functions. The continuity equation is then modified in a consistent way by the addition of a suitable multiple of the divergence of the difference between the pressure gradient and its projection. This Pressure Gradient Projection method (PGP) was proved in [13] to yield stable and optimally convergent approximate solutions of the steady, incompressible Navier-Stokes equations under a weak condition on the approximating finite element spaces; it was shown in [12] that this condition is satisfied by equal order interpolations. A similar technique employed together with a backward Euler temporal approximation was shown in [6] to be stable and convergent for the solution of the transient problem.

It has to be said that other three-dimensional ocean models which employ the finite element method as space discretization scheme use mixed approximations for the velocity and the pressure which satisfy the discrete inf-sup compatibility condition, such as the lowest order Raviar-Thomas element ([10] and [45]), or the MINI element with bubble condensation ([31]). Stabilized formulations have been shown to be more efficient than mixed elements for solving incompressible flow problems (see [38]).

The stabilized method that we consider here is based on a pressure gradient projection and consists in finding $\boldsymbol{u}_h^{n+1} = (u_h^{n+1}, v_h^{n+1}, w_h^{n+1}) \in V_h$, $p_h^{n+1} \in Q_h$, $\eta_h^{n+1} \in M_h$ and $\boldsymbol{r}_h^{n+1} = (r_1^{n+1}, r_2^{n+1}, r_3^{n+1}) \in R_h$, where:

$$R_h \;=\; \{\boldsymbol{s}_h \in (\mathcal{C}^0(\Omega))^3 \;/\; \forall K \in \Omega_h, \boldsymbol{s}_{h|K} = \hat{\boldsymbol{s}}_K \circ F_K^{-1},\; \hat{\boldsymbol{s}}_K \in (R_1)^3\},$$

such that, for all test functions $\tilde{\boldsymbol{u}}_h = (\tilde{u}_h, \tilde{v}_h, \tilde{w}_h) \in V_h$, $q_h \in Q_h$, $\mu_h \in M_h$ and $\boldsymbol{s}_h \in R_h$:

$$\begin{aligned}
\int_\Omega \frac{1}{\Delta t}(\boldsymbol{u}_h^{n+1} - \boldsymbol{u}_h^n)\,\tilde{\boldsymbol{u}}_h\,d\Omega + \int_\Omega (\boldsymbol{u}_h^n \cdot \nabla)\boldsymbol{u}_h^{n+1}\,\tilde{\boldsymbol{u}}_h\,d\Omega \;+\; \int_\Omega (\boldsymbol{k} \times \boldsymbol{u}_h^{n+1})\tilde{\boldsymbol{u}}_h\,d\Omega \\
+ \int_\Omega (\nu_H \frac{\partial \boldsymbol{u}_h^{n+1}}{\partial x}\frac{\partial \tilde{\boldsymbol{u}}_h}{\partial x} + \nu_H \frac{\partial \boldsymbol{u}_h^{n+1}}{\partial y}\frac{\partial \tilde{\boldsymbol{u}}_h}{\partial y} \\
+ \nu_V \frac{\partial \boldsymbol{u}_h^{n+1}}{\partial z}\frac{\partial \tilde{\boldsymbol{u}}_h}{\partial z})d\Omega \;+\; \int_\Omega \nabla p_h^{n+1}\,\tilde{\boldsymbol{u}}_h\,d\Omega \\
= -g\int_\Omega \nabla_2 \eta_h^n\,\tilde{\boldsymbol{u}}_h\,d\Omega \;+\; \int_{\Gamma_s} (\tau_s^x \tilde{u}_h + \tau_s^y \tilde{v}_h)\,d\Gamma \\
+ \int_{\Gamma_b} (\tau_b^x(u_h^{n+1})\tilde{u}_h + \tau_b^y(v_h^{n+1})\tilde{v}_h)\,d\Gamma \\
+ \int_{\Gamma_b} \boldsymbol{n}_\nu \cdot \nabla w_h^{n+1}\,\tilde{w}_h\,d\Gamma, \\
\int_\Omega (\nabla \cdot \boldsymbol{u}_h^{n+1})\,\tilde{q}_h\,d\Omega + \sum_{K\in\Omega_h}\int_K \alpha_K\,\nabla p_h^{n+1}\,\nabla q_h\,d\Omega \\
- \sum_{K\in\Omega_h}\int_K \sqrt{\alpha_K}\,\boldsymbol{r}^{n+1}\,\nabla q_h\,d\Omega \;=\; 0, \\
\int_\Omega \boldsymbol{r}_h^{n+1}\,\boldsymbol{s}_h\,d\Omega - \sum_{K\in\Omega_h}\int_K \sqrt{\alpha_K}\,\nabla p_h^{n+1}\,\boldsymbol{s}_h\,d\Omega \;=\; 0, \\
\int_S \frac{1}{\Delta t}(\eta_h^{n+1} - \eta_h^n)\mu_h d\Gamma + \int_S u_h^{n+1}(\frac{\partial \eta_h}{\partial x})^{n+1}\mu_h d\Gamma \;+\; \int_S v_h^{n+1}(\frac{\partial \eta_h}{\partial y})^{n+1}\mu d\Gamma \\
= \int_S w_h^{n+1}\,\mu_h\,d\Gamma.
\end{aligned}$$

The stabilization coefficients α_K are computed in terms of the size h_K of element K and a characteristic value V_K of the velocity in element K, according to the usual expressions for stabilized formulations (see [21]).

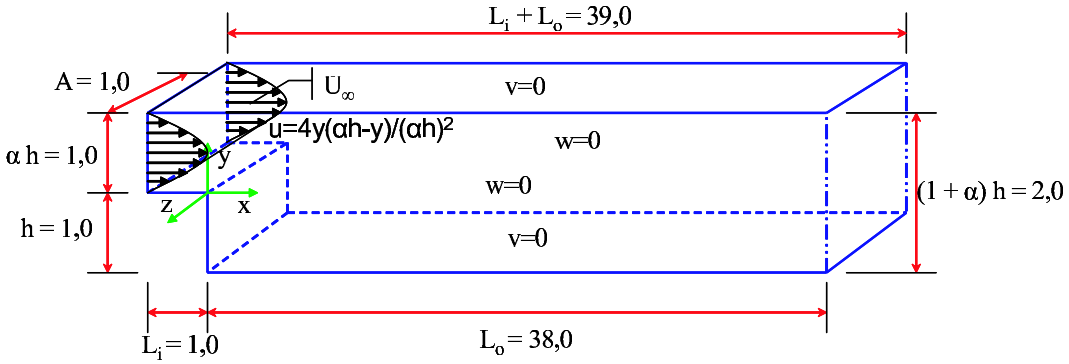

Fig. 1. Backward facing step: geometry and boundary conditions.

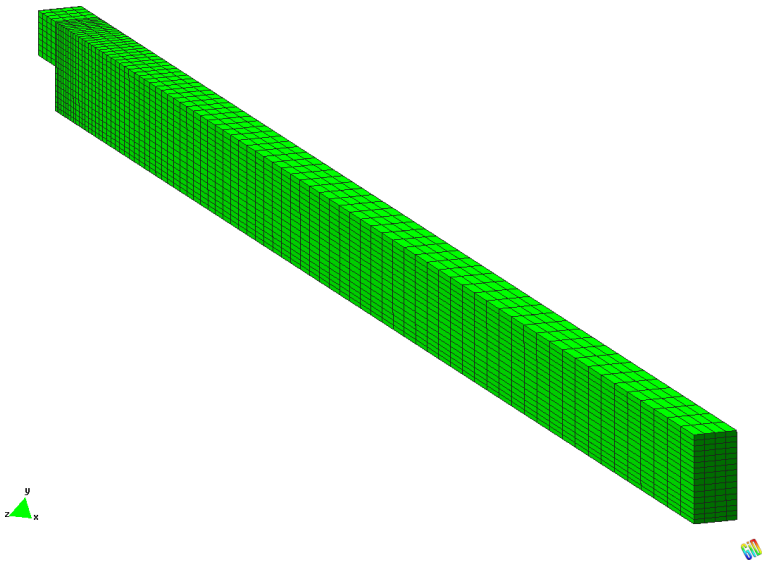

Fig. 2. Backward facing step: three-dimensional mesh.

5 Numerical results

We present in this Section some numerical results obtained with the finite element model presented in the previous Sections.

5.1 Three-dimensional backward-facing step

We first considered the classical problem of the flow over a backward facing step. The geometry of this problem has been employed in many engineering applications such as cooling of electronic devices, heat transfer enhancement of turbine blades and many other heat transfer systems. This case presents complexities such as detachment and reattachment structures which affect the evaluation of the turbulent heat transfer coefficient and thus the heat transfer mechanisms.

Since no buoyancy forces are considered on this flow problem, we tested our model on it for constant values of the viscosity coefficient as well as for the Smagorinsky model. We considered the three-dimensional geometry shown in Figure 1, in which the inlet channel height is 1 and the expansion ratio is 2. The inlet and outlet lengths were, respectively, 1 and 38. A parabolic velocity profile was imposed at the inlet with a maximum velocity of 1, natural boundary conditions were imposed at the outlet and homogeneous Dirichlet conditions were imposed in all other boundaries. To solve this flow problem, we used the mesh of 7065 nodes and 5248 hexahedral elements shown in Figure 2.

Three test cases were considered. The first two ones use constant values of the horizontal viscosity coefficient ν_H corresponding to Reynolds numbers of 600 and 1000 (based on the maximum inlet velocity, the step height and the viscosity); the third one uses the Smagorinsky model for ν_H. In all cases, the vertical viscosity coefficient ν_V was held constant, since no transversal diffusion occurs in this flow problem. A steady state was reached in all cases with a time step size of $\Delta t = 1$s. Figure 3 shows the velocity field obtained in the three cases in the section across $z = 0.5$ (part of the outflow region was left out for clarity reasons); separating and reattaching regions can be observed. These results agree with those of other published numerical solutions, like those of [1]. Figure 4 shows the pressure contours obtained in each case in the same section. The elemental turbulent viscosity coefficients obtained with the Smagorinsky model in the same section as before are plotted in Figure 5.

We compared our solution with the numerical results provided by Gartling in [23] and Barkley *et al* in [1], who solved this problem for Re=600 using two and three-dimensional formulations respectively. The primary reattachment length X_1 is compared to the results of this two references in Table 1. The slightly larger value obtained with the present scheme can be attributed to the poor resolution of the finite element mesh employed in this test case.

Reference	X_1
Gartling ([23])	12,2
Barkley *et al* ([1])	11,91
Present study	12,7

Table 1
Backward facing step: comparison of reattachment length

5.2 Stratified Ekman flow

As a second test case, we considered the Ekman problem for a stratified fluid. The classical Ekman problem consists of the flow of an incompressible fluid

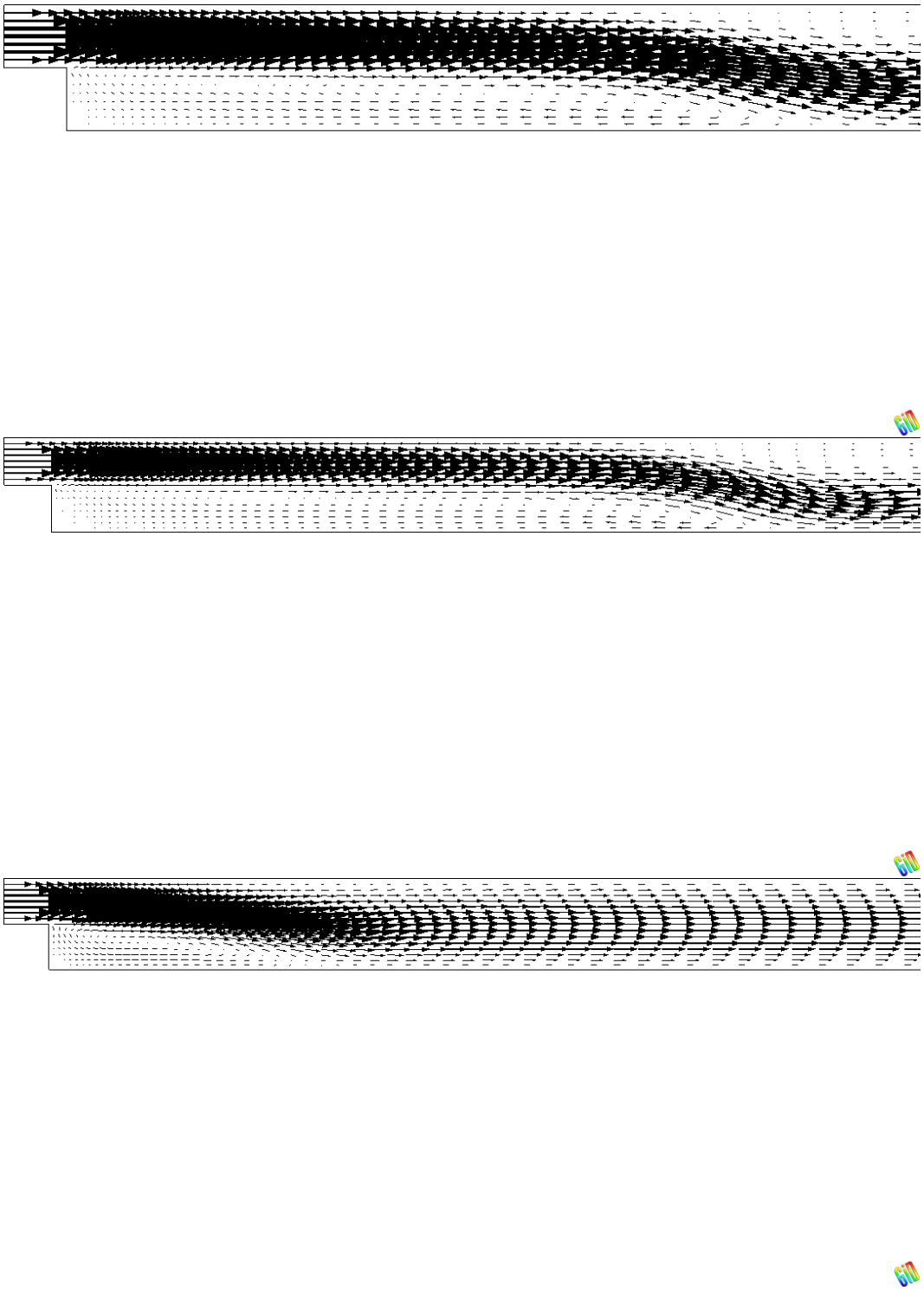

Fig. 3. Velocity vectors in the section $z = 0.5$. Top: $\nu = 0.00166$; middle: $\nu = 0.001$; bottom: Smagorinsky model.

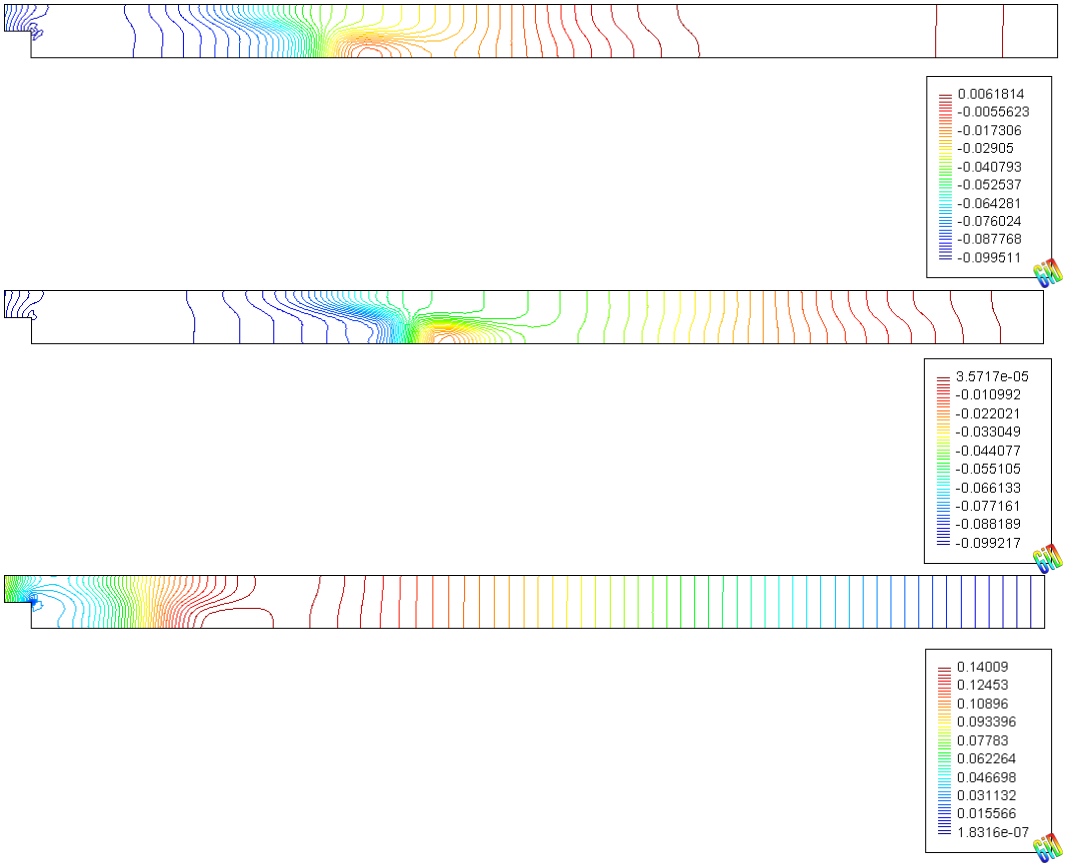

Fig. 4. Pressure contours in the section $z = 0.5$. Top: Re= 0.00166; middle: Re= 0.001; bottom: Smagorinsky model.

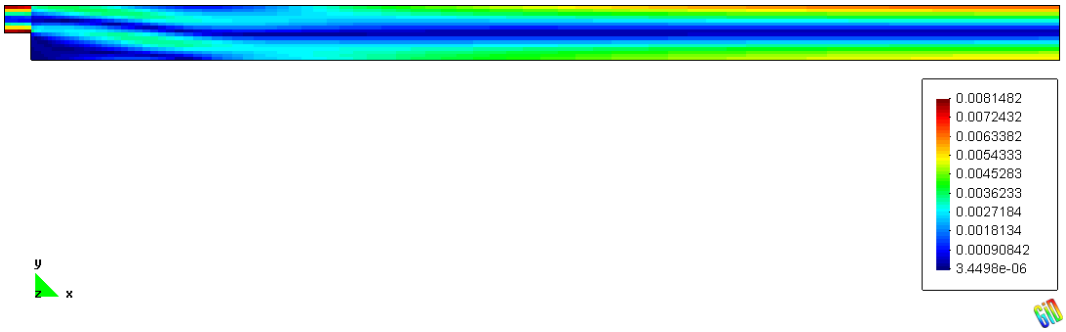

Fig. 5. Turbulent viscosity distribution obtained with the Smagorinsky model in the section $z = 0.5$.

in an ocean of infinite depth driven by a steady wind and subject to the Coriolis force. For a fluid of constant density and constant vertical viscosity, an analytical solution exists (see, for instance, [19]) in which the flow is horizontal, the surface current drifts 45° to the right (in the Northern hemisphere) with respect to the wind direction and the velocity vector decreases exponentially in length with depth while it turns right, thus describing the well-known Ekman's spiral.

We considered the more realistic problem of Ekman's flow in a stratified ocean, a problem for which no analytical solution is available. The density is assumed to decrease linearly with depth, from a value of $\rho = 1000\, Kg/m^3$ at the surface to $\rho = 1024\, Kg/m^3$ at a depth of $100m$. This stratified flow problem is suitable to compare the performance of the different models for the vertical turbulent viscosity coefficient ν_V.

We solved this problem on a cubic domain of side $100m$ with the following values of the physical parameters: latitude $\phi = 45°$, Earth's rotation angular velocity $\omega = 7.292 \cdot 10^{-5}\, s^{-1}$, gravity acceleration $g = 9.81 m/s^2$, air density $\rho_a = 1.3\, Kg/m^3$ and wind drag coefficient $C_s = 1.4 \cdot 10^{-3}$. We considered a steady wind of $10m/s$ in the y-direction. A non-uniform mesh of hexahedral elements with $4 \times 4 \times 30$ elements was employed which is equally spaced in the horizontal directions and refined vertically near the surface and the bottom. We performed the computations with $\Delta t = 10s$ starting from the fluid at rest until a steady state was reached, with a steady state tolerance of 10^{-3}.

Table 999 shows the number of time steps and the CPU time required to reach a converged solution in each of the four cases analyzed: a constant turbulent viscosity $\nu_V = 10^{-2}$, Pacanowski-Philander's model, Munk-Anderson's model and Gent's model (a constant value of $\nu_H = 10^3$ was taken in all cases). Similar computational effort was required in the four cases.

Model	Time steps	CPU time
Uniform	1629	15'11"
Pacanowski-Philander	1633	15'02"
Munk-Anderson	1629	15'35"
Gent	1633	15'18"

Table 2
Stratified Ekman flow: number of time steps and CPU time to reach a steady state.

The steady state results obtained for the column of water at the center of the domain are shown in Figure 6, where we plot the vertical profile of the velocity in the (u, v) plane. Pacanowski-Philander's and Gent's models provide similar but not the same results, despite the similarity of the two formulations. On the other hand, the results of Munk-Anderson's model are close to those obtained with a uniform viscosity distribution. The same drift in the surface current is observed in all four cases.

In Figure 7 we plot the vertical distribution of the vertical turbulent viscosity obtained with each of the three turbulence models employed. Munk-Anderson's is clearly more dissipative than the other two models, a fact which is also reflected in the smaller surface current values obtained with this model and observed in Figure 6.

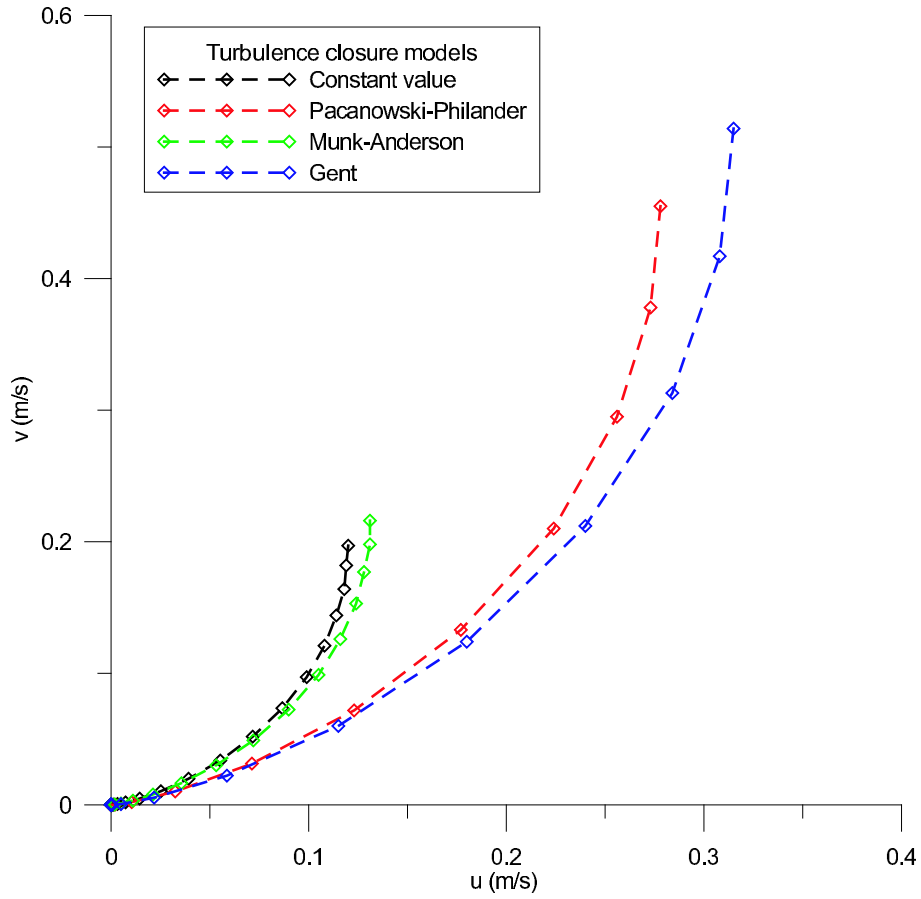

Fig. 6. Stratified Ekman flow: vertical profile of the velocity.

6 Conclusions

A three-dimensional finite element model for turbulent coastal ocean flows has been developed which incorporates different algebraic turbulence models. Both a homogeneous distribution and the LES Smagorisnky models for the horizontal turbulent viscosity coefficient have been employed successfully on a test problem. On the other hand, a constant value and different flow dependent formulations, both classical and recent, have been compared in a stratified flow situation; Munk-Anderson's model has been found to be more dissipative than Pacanowski-Philander's and Gent's models.

References

[1] D. Barkley, M.G.M. Gomes, R.D. Henderson, Three-dimensional instability in flow over a backward facing step, Journal of Fluid Mechanics 473 (2002) 167-190.

[2] Y. Bazilevs, V.M. Calo, J.A. Cottrell, T.J.R. Hughes, A. Reali, G.

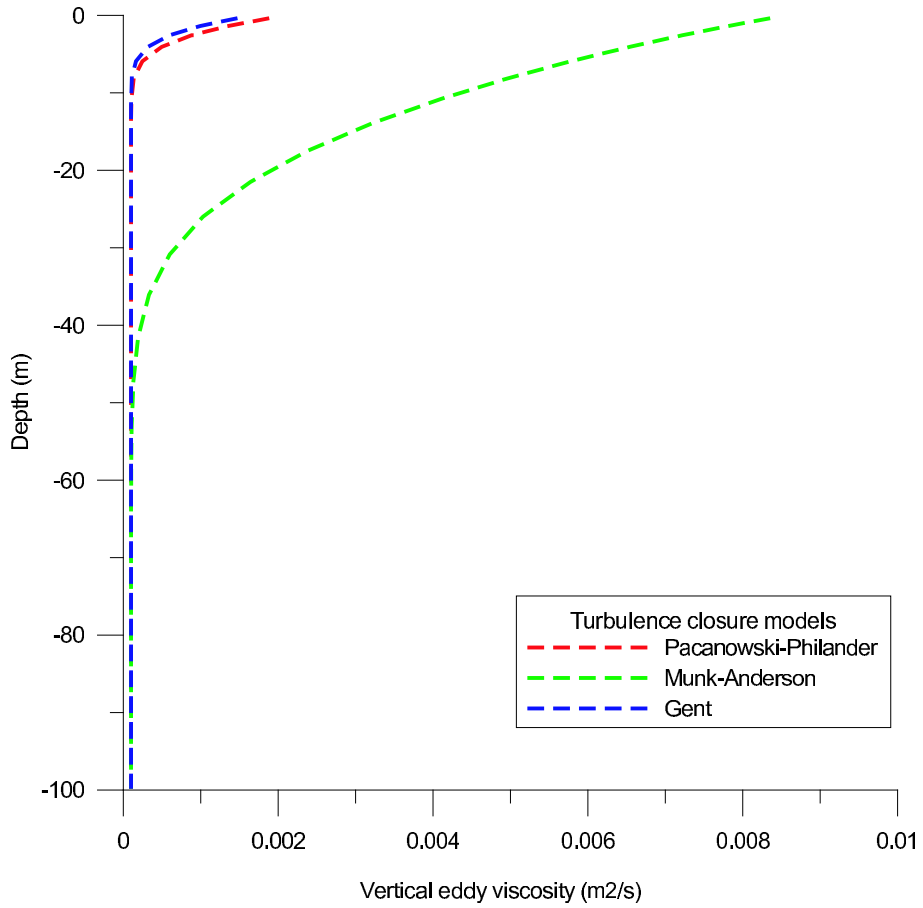

Fig. 7. Stratified Ekman flow: vertical turbulent viscosity distribution.

Scovazzi, Variational multiscale residual-based turbulence modeling for large-eddy simulation of incompressible flow, Computer Methods in Applied Mechanics and Engineering 197 (2007) 173-201.

[3] A.C. Bennis, T. Chacón Rebollo, M. Gómez Mármol, R. Lewandowski, Stability of some turbulent vertical models for the ocean mixing boundary layer, Applied Mathematics Letters 21 (2008) 128-133.

[4] J. Berntsen, E. Svendsen, Using the SKAGEX dataset for evaluation of ocean model skills, Journal of Marine Systems 18 (1999) 313-331.

[5] J. Blasco, An anisotropic pressure-stabilized finite element method for incompressible flow problems, Comp. and Math. with Applications 53 (2007) 895-909.

[6] J. Blasco, R. Codina, Space and time error estimates for a first order, pressure stabilized finite element method for the incompressible Navier-Stokes equations, Applied Numerical Mathematics 38 (2001) 475-497.

[7] J. Blasco, M.A. Maidana, M. Espino, A fully 3D finite element model for non-hydrostatic coastal flows with a free-surface, submitted.

[8] A.F. Blumberg, G.L. Mellor, A description of a three-dimensional coastal ocean circulation model, (N. Heaps ed., American Geophysical Union, 1987.).

[9] V. Casulli, P. Zanolli, Semi-implicit numerical modelling of nonhydrostatic free–surface flows for environmental problems, Mathematical and Computer Modelling 36 (2002) 1131–1149.

[10] P. Causin, E. Miglio, F. Saleri, Algebraic factorizations for 3D non-hydrostatic free surface flows, Computing in Visualization and Science 5 (2002) 85–94.

[11] T. Chacón Rebollo, D. Rodríguez Gómez, A stabilized space-time discretization for the primitive equations in oceanography, Numerische Mathematik 98 2004 427–475.

[12] R. Codina, J. Blasco, A finite element formulation for the Stokes problem allowing equal velocity-pressure interpolation, Computer Methods in Applied Mechanics and Engineering 143, 3-4 (1997) 373-391.

[13] R. Codina, J. Blasco, Analysis of a pressure-stabilized finite element approximation of the stationary Navier-Stokes equations, Numerische Mathematik 87 (2000) 59-81.

[14] R. Codina, J. Blasco, Stabilized finite element method for the transient Navier-Stokes equations based on a pressure gradient projection, Computer Methods in Applied Mechanics and Engineering 182, 3-4 (2000) 277-300.

[15] A.M. Davies, P. Hall, A three-dimensional model of diurnal and semidiurnal tides and tidal mixing in the North Channel of the Irish Sea, Journal of Geophysical Research 105 (2000) 17,079–17,104.

[16] S. Danilov, G. Kivman, J. Schröter, A finite–element ocean model: principles and evaluation, Ocean Modelling 6 (2004) 125–150.

[17] C. Dawson, J. Proft, Coupled discontinuous and continuous Galerkin finite element methods for the depth-integrated shallow water equations, Computer Methods in Applied Mechanics and Engineering 193 2004 289–318.

[18] A. Deponti, V. Pennati, L. De Biase, A fully 3D finite volume method for incompressible Navier-Stokes equations, International Journal for Numerical Methods in Fluids 852 (2006) 617–638.

[19] N.I. Egorov, Oceanografía Física, Vneshtorgizdat, (MIR, Moscow). 1983

[20] M. Espino, M.A. Maidana, A. Sánchez-Arcilla, A. German, Hydrodynamics in the Huelva Estuary: tidal model calibration using field data, Journal of Waterway, Port, Coastal and Ocean Engineering 133 (2007) 313–323.

[21] L.P. Franca, T.J.R. Hughes, Convergence analyses of Galerkin least–squares methods for symmetric advective–diffusive forms of the Stokes and incompressible Navier–Stokes equations, Computer Methods in Applied Mechanics and Engineering 105 (1993) 285-298.

[22] P.R. Gent, The heat budget of the toga-coare domain in an ocean model, Journal of Geophysical Research 96 (1991) 3323-3330.

[23] D.K. Gartling, A test problem for outflow boundary conditions - flow over a backward-facing step, International Journal for Numerical Methods in Fluids 11 (1990) 953-967.

[24] S.M. Griffies, R.W. Hallberg, Biharmonic friction with a Smagorinski viscosity for use in large-scale eddy-permitting ocean models, Monthly Weather Review 128 (2000) 2935-2946.

[25] F. Guillén-González, D. Rodríguez-Gómez, Bubble finite elements for the primitive equations of the ocean, Numerische Mathematik 101 2005 689–728.

[26] D.B. Haidvogel, H.G. Arango, K. Hedstrom, A. Beckmann, P. Malanotte-Rizzoli, A.F. Shchepetkin, Model evaluation experiments in the North Atlantic Basin: simulations in nonlinear terrain-following coordinates, Dynamics of Atmospheres and Oceans 32 (2000) 239-281.

[27] T.J.R. Hughes, Multiscale phenomena: Green's function, the Dirichet-to-Neumann formulation, subgrid scale models, bubbles and the origins of stabilized formulations, Computer Methods in Applied Mechanics and Engineering 127 (1995) 285-298.

[28] T.J.R. Hughes, G.R. Feijóo, L. Mazzei and J.B. Quincy, The variational multiscale method- a paradigm for computational mechanics, Computer Methods in Applied Mechanics and Engineering 166 (1998) 3-24.

[29] T.J.R. Hughes, L. Mazzei, K.E. Jansen, Large-eddy simulation and the variational multiscale method, Computing and Visualization in Science 3 (2000) 47-59.

[30] M.B. Koçyigit, R. A. Falconer, B. Lin, Three-dimensional numerical modelling of free surface flows with non-hydrostatic pressure, International Journal for Numerical Methods in Fluids 40 (2002) 1145–1162.

[31] R.J. Labeur, J.D. Pietrzak, A fully three dimensional unstructured grid non-hydrostatic finite element coastal model, Ocean Modelling 10 (2005) 51–67.

[32] W. Large, P.R. Gent, Validation of vertical mixing in an equatorial ocean model using large eddy simulations and observations, Journal of Physical Oceanography 105 (1993) 285-298.

[33] P. Lin, C.W. Li, A σ-coordinate three-dimensional numerical model for surface wave propagation, International Journal for Numerical Methods in Fluids 38 (2002) 1045–1068.

[34] P.J. Luyten, E. Deleersnijder, J. Ozer, K.G. Ruddick, Presentation of a family of turbulence closure models for stratified shallow water flows and preliminary application to the Rhine outflow region, Continental Shelf Research 16 (1996) 101-130.

[35] A. Mahadevan, J. Oliger, R. Street, A non-hydrostatic mesoscale ocean model. Part I: Well-posedness and scaling, Journal of Physical Oceanography 26 (1996) 1868–1880.

[36] M.A. Maidana, J.J. Naudin, M. Espino, M.A. García, A. Sánchez-Arcilla, Feasibility and usefulness of diagnostic calculations of the mean circulation in the vicinity of the Ebro mouth. Model tests against field data, Continental Shelf Research 22 (2002) 229–245.

[37] W. H. Munk, E. R. Anderson, Notes on a theory of the termocline, Journal of Marine Research 7 (1948) 276–295

[38] S. Norburn and D. Silveser, Stabilized vs. stable mixed methods for incompressible flows, Computer Methods in Applied Mechanics and Engineering 166 (1998) 131-141.

[39] P. Ortiz, O.C. Zienkiewicz, J. Szmelter, Hydrodynamics and transport in estuaries and rivers by the CBS finite element method, International Journal for Numerical Methods in Engineering 66 2006 1569–1586.

[40] R. C. Pacanowski, S. G . H. Philander, Parameterization of vertical mixing in numerical models of tropical oceans, Journal of Physical Oceanography 11 (1981) 1443–1451

[41] B.C. Roisin, Introduction to geophysical fluid dynamics, (Englewood Cliffs, New Jersey 07632, Dartmouth College, 1994).

[42] J. Pedloski, Geophysical fluid dynamics, (Springer, 2nd. Edition, 1987).

[43] J. Smagorinsky, General circulation experiments with the primitive equation: I. The basic experiment, Monthly Weather Review 91 (1963) 99–164

[44] J. Smagorinsky, Large eddy simulation of complex engineering and gepphysical flows. Some historical remarks on the use of nonlinear viscosities, (Cambridge University Press. B. Galperin and S.A. Orszag (Eds.), 1993).

[45] R.A. Walters, Coastal ocean models: two useful finite element methods, Continental Shelf Research 25 (2005) 775–793.

[46] J. Xing, A.M. Davies, Application of a range of turbulent energy models to the determination of M_4 tidal current profiles, Continental Shelf Research 16 (1996) 517–547.

[47] H. Yuan, C.H. Wu, A two-dimensional vertical non-hydrostatic σ model with an implicit method for free-surface flows, International Journal for Numerical Methods in Fluids 44 (2004) 811–835.

[48] O.C. Zienkiewicz, P. Ortíz, A split-characteristic based finite element model for the shallow water equations, International Journal for Numerical Methods in Fluids 20 1995 1061–1080.